Analysis of Grain Size Distribution for samples from the North Caspian Sea Basin

Stephanie Lier
January 2010

1. Introduction

This project is part of a more extensive research project conducted by F. Ernens and supervised by R.M. Hoogendoorn, which focuses on analyzing and interpreting the sedimentary systems of the North East Caspian Sea. One of the main bases for the research of this project is a collection of cores retrieved from five boreholes in the North East Caspian Sea, off the coast of Kazakhstan.

The ultimate goal of this project is to identify the controls of the sedimentary systems of the North East Caspian Sea, in order to improve the capabilities for the assessment of the effects of the construction of future installations in the vicinity of Karain and Aktote islands on the coastal dynamics. Additionally, we want to enable comparative analyses and the selection of more environmentally acceptable route of the future sealines/pipelines therefore assisting the planning of future production facilities such as artificial islands, platforms and pipelines.

Grain size analysis is important in this context for several reasons. Not only is it a basic descriptive measure of the sediment, but it can also be characteristic of sediments deposited in certain environments. It may also tell us about additional properties such as the physical mechanisms acting during transportation and deposition or the permeability of the sediment.

In order to obtain this information, cores from five separate boreholes (see Fig. 1) were taken from the North Eastern Caspian Sea and analyzed. This was done using a Hiac Royco Model 3000, which employs the light blocking method of particle counting.

This report will discuss both the geology of the region and the various methods for particle size counting; and explain the choice for the light blocking method. Finally, the results of the analysis will be presented and interpreted.

2. Regional geology

The North Caspian Basin was formed in a rift zone as part of the Pre-Caspian Basin. It is generally accepted that rifting took place sometime between the Late Proterozoic and Middle Devonian. The spreading resulted in the formation of oceanic crust that forms the deep basement of the current basin.

The basin developed independently from the world oceans from the Mid Pliocene on. However, due to a series of transgressions, occasional links with the world oceans were established and during subsequent regressions these links were terminated. These dynamics persistently changed the size, salinity and biological population of the basin. (Verlinden and Hoogendoorn, 2009)

Four major transgressive stages can be distinguished during the late Quaternary: Bakunian, Khazarian, Khvalynian and Neocaspian. (Leont'ev and Fedorov, 1953; Kosarev and Yablonskaya, 1994; and others). At maximum highstand stages pronounced shorelines developed, thus shaping a distinctive coastal morphology (Leont'ev, Maev and Rychagov, 1977). Alternatively, regressions caused the marine basin to shrink, leaving large parts of the North Caspian basin sub-aerial exposed and subject to erosion. The coastal zone of the Northeastern Caspian Sea can be divided into four general areas: coastal plains, mud flats, a reed-bed barrier zone and the open shallow Caspian Sea.

Three major rivers flow into the Caspian Sea, with the Volga by far the largest, supplying approximately 80% of the total water supply to the Caspian Sea. The remaining two rivers are the Ural and the Emba.

Krushtalov and Ryshkov (1975) concluded that sediments of the western part of the North Caspian Sea, around the Volga River delta are logically the results from discharge of terrigenous material by the Volga River. The sediments in the Ural Furrow and around the Ural delta are mainly Ural River sediments and of lesser importance, Volga River sediments, Aeolian sediments and suspended material from the Western half of the Northern Caspian. The eastern part of the North Caspian Sea, south and east of the Ural Furrow are mainly controlled by the supply of terrigenous material from Aeolian sediments from the Buzachi Peninsula. Large area to the east part of the North Caspian near the Emba River have been attributed to the Emba River indicating a strong outflux of sediment from this river in the past. (Khrustalev and Ryshkov 1975)

In studying the cores, for different lithological facies could be distinguished:

Unit	Facies name	Approx. depth below seafloor	Description	Depositional environment
1	Grey sands	0-1 m	*Fine to coarse sands with shell debris and gypsum bands*	Shoreface
2	Brown sands	1-4 m	*fine to medium layered sands with small shell fragments*	Barrier
3	Silty clays	4-9 m	*Olive grey silty clay with organic rests and gypsum bands*	Lagoon
4	Overconsolidated sands	> 9 m	*Fine to medium sands with small shell fragments*	Undetermined

The overconsolidated sands were only found in 3 of the cores. They were badly sorted and contained bands with small shell fragments. The sedimentology of these sands would point to a coastal depositional environment. However, the seismic reflection of these sands in the Kashagan area and in the whole area between the Kashagan to Karain cluster, show E-W oriented channel-like shapes on maps interpreted from shallow seismics. The shapes, sizes and distribution of the channel-like patterns have much more in common with the onshore longitudinal ridges that are interpreted as Aeolian-dune deposits. Such deposits can be found in the whole onshore North Caspian region and are known as Baer knolls. The shapes, sizes and E-W orientation of the Baer knolls are similar to the features on the seismic images. It is more likely that these features were deposited as longitude Aeolian dunes during a lowstand on the exposed seabed. (Verlinden and Hoogendoorn, 2009)

3. Methods of Particle Counting

There are many different methods of particle counting, each with their own advantages and disadvantages. Methods for particle counting include laser diffraction, based on the light scattering properties of differently sized particles; sedimentation, based on the settling velocity of differently sized particles; electroresistance particle counting, based on the volume of electrolyte of differently sized particles; time of transition, which counts the particles using a rotating laser beam; dry sieving, in which the samples are put through various sieves and the resulting fractions are measured; and image analysis, which uses software to measure the geometric properties of particles on photographs or other surfaces. (Goossens, 2006)

None of these methods, nor any other method, can be perceived as being perfect and the results obtained from the various methods can differ significantly. This can be due to various factors: it can be due to the effects of particle shape, but also due to the way in which the data is interpreted by computer software. Another factor is the definition of grain-size: Techniques based on different physical principles define grain-size in different ways. (Blott, 2006)

The type of sediment, of course, also plays a role. Different types of sediments will yield different results, due to their respective difference in factors such as density, flattening, angularity, etc. In image analysis, for instance, the only sediments that should be considered are those in which the separate particles are readily identifiable. On the other hand, image analysis does not require the extraction and alteration of the sample by means of preparation and analyzing, which allows for minimal distortion of the source data. (Goossens, 2008)

Practical factors should also be considered. For instance, in order to obtain optimal results, an analysis should have high reproducibility. Techniques based on laser diffraction or sedimentation, which consider more particles than other techniques, have an advantage in this area. However, the reproducibility is also significantly affected by the complexity of the experimental protocol. More complexity means a higher risk of experimental error, which could have a significant effect on the results. Generally speaking, a technique should be as simple as possible to operate; the complexity of the calculations should be as low as possible, a significant amount of sediment should be used and the technique should cost a minimum amount of time. (Goossens, 2008)

There is no single technique that ticks all of these boxes, so the various possibilities should be considered for each separate set of samples.

In this case, we made use of a light blockage particle counter. This technique was first introduced in the 1960s and operates under a simple principle: a

beam of light is projected through the sample fluid; if a particle blocks the light, it results in a measurable energy drop that is roughly proportional to the size of the particle (see Fig. 2).

This technique has several advantages. With a particle count of 1000 – 18000 counts per ml, the sampling size is fairly large, and the counter is able to measure a sample of 8 ml within 20 seconds. Given that the machine does almost all of the work, the reproducibility is fairly high. Using a single macro to do the further calculations for all of the results means minimal error on that front. However there is some room for error during the preparation of the sample, and the data obtained from the machine still need to be interpreted. Due to a risk of clogging, the particles cannot be bigger than 0.3 mm, but this is easily remedied by sieving the samples, although in our case, this was hardly necessary to begin with.

4. Procedure

Two days of preparation were required before each sample could be measured. First all of the moisture needed to be removed from the sample. This was achieved by leaving the samples overnight in an oven heated to about 105ºC. The samples were weighed before being put in the oven and after they were taken out, so as to get an impression of the moisture content of the sample. The results of these measurements can be found in the appendix.

Next, the samples were ground using a mortar and pestle. This proved to be easy for most of the sandy samples, but a lot tougher for some of the finer sediments. Once the sample had been ground to a level where the grains were separated from one another, about 0.5 grams of each sample were weighed and put into 800 ml glass beakers.

After adding a small amount of distilled water to the samples, they were heated up and oxidized using aliquots of 5 ml of 30% H_2O_2. If there was a violent reaction, which there usually was for the finer sediments, more H_2O_2 was added. For most of the sandy sediments, just 5 mls of H_2O_2 was sufficient.

Once the peroxide had been added, the samples were filled up to 100 ml with demineralized water and left to boil for about 10 minutes or more; in some cases more water was added to avoid boiling to dryness.

After letting the samples cool down to 40ºC or less, they were treated with 10% HCl in similar 5 ml aliquots in order to eliminate the carbonate content. Once there was no more violent reaction, the samples were again heated to boiling point for no more than one minute. After cooling down, they were filled to the top with distilled water and left to stand overnight.

The next day, the samples were first decanted down to about 50 ml. They were then put through a sieve of 0.3 mm to remove oversize particles, although the sample volume was generally too small to warrant a large amount of residu in the sieve. Finally, in order to stimulate dispersion of the particles, 300 mg $Na_4P_2O_7.10H_2O$ was added to each sample, before heating it to boiling point for one more minute.

After this preparation, the samples were ready to be measured with the particle counter. The particles were first brought into suspension using a magnetic stirrer and a stirring bar. A small sample was then taken of the suspension, generally about 1 – 10 ml, depending on the type of sediment. This sample was then filled to 200 ml with distilled water and measured using the particle counter. Depending on the resulting amount of counts per ml, the sample was then diluted or concentrated accordingly. The number of counts per ml was to be between $1.0 \cdot 10^4$ and $1.8 \cdot 10^4$.

The particles were counted using a Hiac Royco Model 3000, with a sample volume of 8 ml. Once the desired amount of counts per ml was reached, five additional runs were done for a total of six measurements per sample.

After the measurement, the data were converted from SIZ format to ASC format and then exported using a 3.5-inch floppy disk. The data were entered into Excel and processed using a macro which produces a clear graph of the particle counts on the ϕ–scale, the results of which can be viewed in the appendix.

5. Results

After measuring the samples with the particle counter, the results were processed in Microsoft Excel in order to obtain a graph of the counts versus the particle size on a logarithmic φ-scale. This scale is a logarithmic transformation of the Udden-Wentworth scale (1922), proposed by Krumbein in 1934 (see Table 1). It is usually accepted that size should be measured on some type of geometric or logarithmic scale because, for example, a change from 1 to 2 mm is obviously a more significant change in size than a change from 101 to 102 mm. (Blatt, Middleton and Murray, 1980)

Although every sediment is different, some general rules have been set by Friedman (1961, 1967) with regards to the grain size distribution of various typical depositional environments. He found, for instance, that beach sands can be recognized by their combination of negative skewness and good sorting. River sands, however, tend to be positively skewed and less well sorted. Coarse river sands may be negatively skewed. Dune sands have positive skewness and are usually somewhat finer grained than beach sands. The skewness in river sands, however, has a different cause than the skewness in dune sands: whereas in river sands the skewness is due to a fine tail, caused by the presence of suspended clay and silt in the river water, the skewness in the dune sands is caused by truncation of the coarse tail due to the fact that the wind is unable to move the coarse sands. (Blatt, Middleton and Murray, 1980)

In an aeolian environment, the larger grains generally roll around in the aeolian source area to form desert sand, whereas the smaller grains, mainly silt and clay, are transported away from the source area in suspension to be deposited in either adjacent or quite distant areas to form loess. Further investigations on Aeolian particle dynamics have found that the coarse grain population, or silt fraction in Aeolian sediments, is generally transported by surface winds and moves from one site to the next, step by step, in short suspension episodes. This coarse Aeolian population massively accumulates in the downwind adjacent areas to form loess. Conversely, the fine-grained population, or clay fraction, once injected off the ground, can be dispersed within a wide altitudinal extent and is mainly transported by upper level air flow to be deposited in distant areas. Therefore, desert regions, like northwestern China, preserve a coarse altation and suspension population, and the loess areas adjacent to the desert source regions receive both coarse and fine Aeolian populations, whereas the distant areas like the Northern Pacific Ocean can only receive the fine one. (Sun, Bloemendal et al., 2002)

Although the results are generally conform to what we would expect from the lithostratigraphy, there are some slight variations, which could be caused by any number of experimental errors. An overview of the graphs derived from the measurements can be found in the appendix. The corresponding lithostratigraphic columns can also be found there, in figs. 3-7. From the results we can draw conclusion both about the vertical and the lateral correlations between the bodies of sand. Both will be discussed here.

5.1 Vertical interpretation

CDS-A

The first and only sample in borehole A for the grey sands is the first one, at 0.05 m, with a peak at 3 on the ϕ-scale, which indicates fine sand. The next core is at 2 m, where we find the brown sands with fluctuating amounts of fine vs. coarse material, but generally with two peaks: one at 3.5 on the ϕ-scale and one at 5.5 on the ϕ-scale. The two exceptions to this rule are at either end of the facies: at 2.00 m there are two peaks at respectively 6 and 4.5 on the ϕ-scale, and at 3.60 m, there is a peak at 6 rather than 5.5. These fluctuations can be due either to a transitional phase from or to another facies or to the banding that is present in the facies, as can be seen in figure 3.

Starting from 3.95 m, we find the silty clays. These start with a peak at 5, with some material both finer and coarser entering the mix at 4.15 m., which might have something to do with the unconformity that can be seen at that depth in fig. 3. After that there is a consistent peak at 5.5, indicating finer material, until 4.75 m, where some coarser material appears. The coarser material remains until 5.60 m, at which point much finer material, with a consistent peak at 6.5 appears. This is in accordance with the lithostratigraphic column, which shows finer material from that depth onwards. The grain size distribution for the silty clays remains more or less uniform, with some coarser material appearing sporadically.

Starting from 8.00 m, some coarser material clearly starts entering the mix. This is undoubtedly a transitional phase towards the overconsolidated sands, which finally enter the mix starting from about 9.50 m. The fine material at 9.30 m is also explained in the lithostratigraphic column in fig. 3. The overconsolidated sands show two peaks: at 5.5 and 3.5, much like the brown sands. From what we can tell from these two samples, the overconsolidated sands seem to become coarser with depth.

Grey sands at 0.05m (peak at 3)	Brown sands at 3.60 m (peaks at 3.5 and 5.5)	Silty clays at 4.80 m (peak at 5.5)	Overconsolidated sands at 10m (peaks at 3.5 and 6)
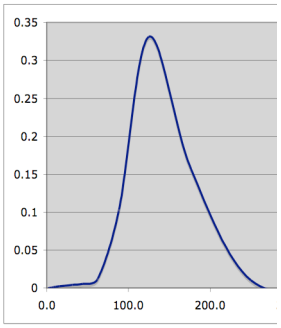	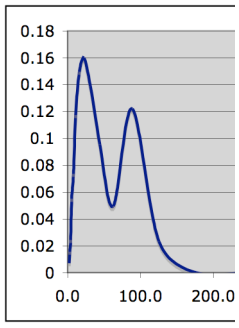	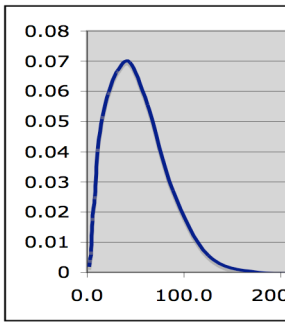	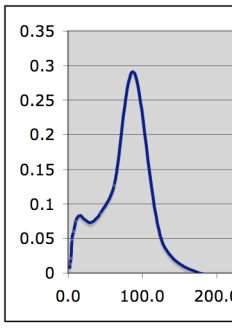

CDS-B

The grey sands in borehole B have a peak at 3.5 on the ϕ-scale which decreases with depth, while the coarse peak (6 – 5.5) seems to increase, which suggests an increase in finer material with depth. The brown sands, starting from 0.90 m, have more or less constant peaks at 3.5, and 6/5.5, the only exceptions being at 1.10m, where there is only a peak at 3.5, and 3.40 m, where there is only a peak at 5.5. In both cases the brown sands are bordering a transitional phase, which probably accounts for these deviations. The amount of coarse material in proportion to finer material fluctuates somewhat within this facies, which can be explained by the banding that can be seen in fig. 4.

We can clearly see the amount of coarse material start to decrease at around 4.80 m, which is where the silty clays start. At 5.90 there is no more coarse material left, and the silty clays remain, with a peak between 6 and 7, until about 8.80 m. At 8.90 we see an abrupt increase in coarse material, with the fines peak at 6.5 almost completely eliminated at 9.10 m. This supports the theory that the overconsolidated sands become coarser with depth.

Grey sands at 0.30m (peaks at 3.5 and 6.5)	Brown sands at 2.70 m (peaks at 3.5 and 5.5)	Silty clays at 5.90 m (peak at 3.5)	Overconsolidated sands at 9.80m (peaks at 3.5 and 6)
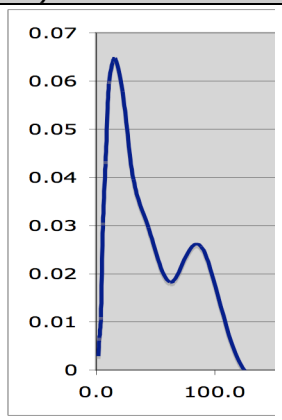	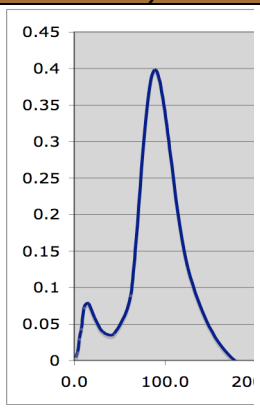	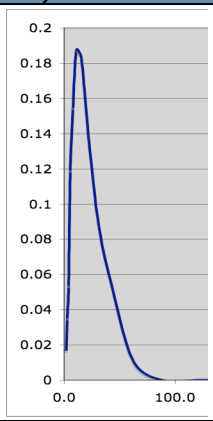	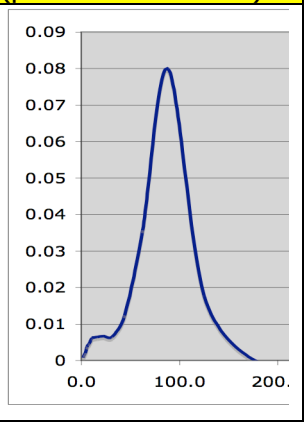

CDS-C

In this borehole the grey sands go quite a bit deeper than they do in boreholes A and B. However they seem fairly consistent, with a peak around 3.5 until 1.20 m, at which point the material becomes coarser with a peak around 5. This might be due to the transition into the brown sands at 2.70 m, or due to the unconformity or banding within the facies.

The brown sands start around 2.70 m, with a fairly consistent peak around 5.5, and some occasional finer material turning up here and there, with more fines turning up with depth. The actual silty clays don't seem to start until about 5.00 m, however, rather than the 4.60 which the lithostratigraphic column suggests. However this could just be a transitional phase. The pure

fine material of the silty clays starts around 5.70, with a peak around 6.5. Some coarser material enters the mix around 7.50 m, which is in accordance with the lithostratigraphic column. At 9.20 m, we can see very clearly that we are approaching the unconsolidated sands, as there is a significant peak in coarse material at that depth. In fact it seems that they might already be present at 9.20, considering the sudden, violent increase in coarse material.

Grey sands at 0.55m (peak at 3.5)	Brown sands at 2.70 m (peak at 5.5)	Silty clays at 7.10 m (peak at 6.5)
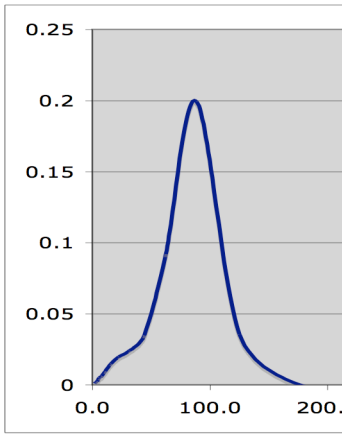	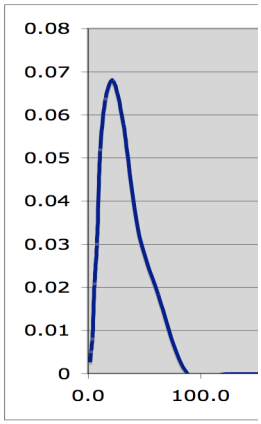	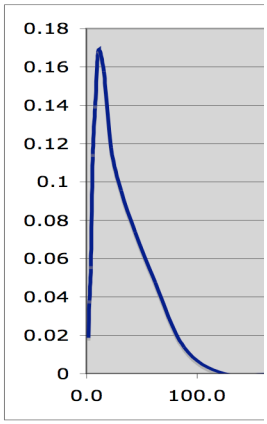

CDS-D

In the D-core we find the grey sands a mix again of peaks around 3.5 and 6. We see the first brown sands at 1.50 m, starting with a fines peak around 6.5, but gradually gaining more coarse material. Between 2.70 m and 3.10 m, there is a slight drop in grain size, which is in accordance with the lithostratigraphic column. After that the grain size is fairly uniform, with consistent peaks around 3.5 and 5.5. The silty clays start around 4.50, with some coarse material at the top in the transition with the brown sands, but quickly reverting to solely a fines peak around 6 from 4.90 m onwards. Although there are no unconsolidated sands in this core, the slight increase in grain size towards the bottom suggests that we are approaching them.

Grey sands at 0.20 m (peaks at 3.5 and 6)	Brown sands at 3.10 m (peaks at 3.5 and 5.5)	Silty clays at 6.80 m (peak at 6.5)
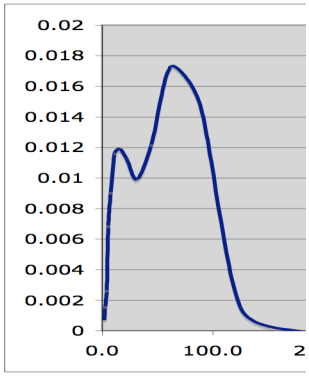	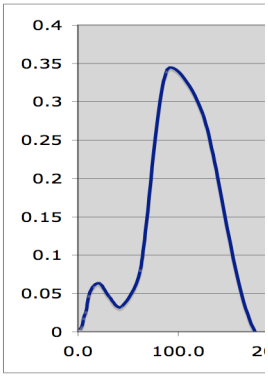	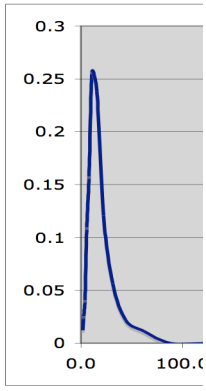

CDS-F

The grey sands in core F seem to share a common peak at around 5. At 1.30 we can first see the brown sands, at first with some fine material, but gradually gaining in coarse material until there is hardly any fine material left at 2.70 m. From there until 4.10 m there is a gradual increase in fines, which makes sense as the silty clays start at around 4.20 m. These once again have a fines peak around 6, but the clays in this borehole also contain some coarser material between 5.30 and 6.50 m. The lithostratigraphic column shows us a different layer between these depths.

Further on the clays show more or less consistent fines peaks around 6, with some coarser material entering between 8.40 and 9.20 m. This could be due to the extensive banding of the matertial at that depth.

At 9.75 m, the material is still very fine, which suggests that the overconsolidated sands are still quite a bit further down.

Grey sands at 0.60 m (peak at 5)	Brown sands at 3.20 m (peaks at 3 and 5.5)	Silty clays at 6.50 m (peak at 6)
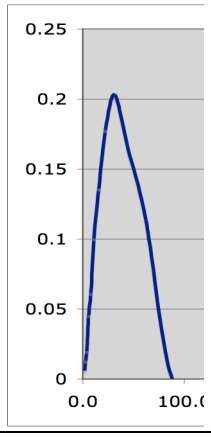	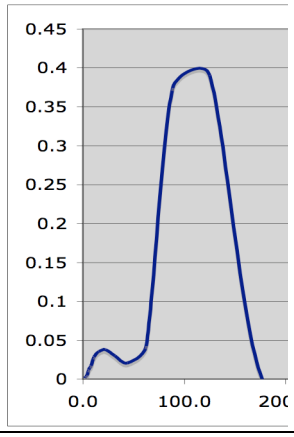	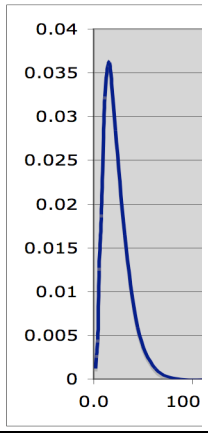

5.2 Lateral interpretation

If we look at the location of the boreholes (Fig. 1), we can see that boreholes A and B are at more or less the same latitude, with A more to the east and B more to the west. The same goes for boreholes C and D, with borehole C being more towards the east. Finally, borehole F is located towards the southwest of all these boreholes.

To determine the lateral correlation between the sand bodies, I will therefore first compare the results from borehole A and B with each other, to see what the fluctuation in an E-W direction is then C and D, and finally compare both these results with borehole F, to determine the fluctuations along the N-S direction.

Grey Sands

It is difficult to draw parallels between the grey sands in boreholes A and B because there is just one sample of grey sands in borehole A.

In borehole C, the grey sands start out with peaks at 3.5 and 5.5, but ends up with just the finer peak. We see some slightly finer material in borehole D, but there, too, we find coarse material with a peak at 3.5. However, in borehole F, we find almost exclusively fine material.

This would seem to indicate that the material becomes finer towards the south; however this is difficult to confirm because the only borehole with a significant amount of data about this layer is borehole C. However, if this is the case, it would indicate a shoreface depositional environment in which the coarse material is deposited closer to shore and the finer material is deposited further out in the sea. Since this is the answer we are expecting to find, it seems like a reasonable assumption.

Brown sands

The brown sands in boreholes A, B, D and F all seem to contain predominantly coarse material. However the material in borehole C is a lot finer. Since the material was deposited in a coastal barrier environment, it might be possible that boreholes A, B, D and F lay within the barrier and borehole C lay outside it. However this does not seem likely because the other boreholes all have a relatively similar grain size distribution.

Silty clays

The grain size distribution of the silty clays, too, is relatively uniform, although the clays in borehole A and C do contain more coarse material. Overall, however, they seem to have been deposited in a similar depositional environment, probably with the shore being on the east side, closest to boreholes A and C which contain the coarser material.

Unconsolidated sands

Comparing boreholes A and B, there does not seem to be much difference between the unconsolidated sands: they both start out with some finer

material, but increase in coarseness with depth. Unfortunately there is not a lot of data to go on with regards to these sands. However the accumulation of coarse material, with almost complete elimination of the fine material (and probably complete elimination with an increase of depth), does seem to support the possibility of an Aeolian depositional environment.

However, when we look at the actual coarseness of the grains, although they are still classified as fine grains on the φ-scale, they are still among the coarsest sands in the borehole. This seems to contradict our expectation that Aeolian sands would be slightly finer-grained than beach sands. And since we already have other sands in the borehole with a similar grain size distribution, it might be just as likely that the sands have a water-transported origin.

6. Discussion

Although there are countless methods for particle counting, it is important to weigh all the factors in each particular case before deciding which method is the most suitable for the current situation. In this case, the laser blocking method was adequately suited to our purposes, particularly because the material that was being measured was relatively fine – so fine, in fact, that the sieve yielded hardly any residue at all, for any of the samples. Moreover, because the process is almost entirely automated, the accuracy is high and the room for error small. Unfortunately the room for error cannot be completely eliminated, particularly during the preparation phase where a mistake is easily overlooked.

Thankfully, however, the results obtained seem satisfactory. The grey sands turned out to be relatively coarse-grained, with the brown sands more of a mix between fine and coarse material, the silty clays fine, and the unconsolidated sands coarse, and probably even coarser as depth increases. It is unfortunate that there is so few data precisely of the sands we want to know more about: the unconsolidated sands of possible Aeolian origin. However this might be easily solved by retrieving more data from the North Caspian Basin.

7. Conclusion

With regards to the depositional environments of the grey sands, brown sands and silty clay, these analyses support what we already know. Unfortunately there is simply not enough data on the unconsolidated sands to draw any definitive conclusions about its depositional environment. However none of the hypotheses about the origin of the sediment – be it fluvial, coastal or aeolian – are contradicted by these results and, if additional data can be found, it is possible that grain size analysis may aid in the determination of the origin of the sands.

8. Literature

Blatt, H., Middleton, G. & Murray, R., *Origin of Sedimentary Rocks*, Prentice-Hall, New Jersey (1980), pp. 43 – 89

Blott, S. & Pye, K, Sedimentology **53** (2006), pp. 671-685:
Particle size distribution analysis of sand-sized particles by laser diffraction: an experimental investigation of instrument sensitivity and the effects of particle shape

Bui, E., Mazzullo, J. & Wilding, L., Earth Surface Processes and Landforms **14** (1989), pp. 157-166:
Using quartz grain size and shape analysis to distinguish between Aeolian and fluvial deposits in the Dallol Bosso of Niger (West Africa)

Buscome, D. & Masselink, G., Sedimentology **56** (2009), p.p. 421-438:
Grain-size information from the statistical properties of digital images of sediment

Goossens, D., Sedimentology **55** (2008), pp. 65-96:
Techniques to measure grain-size distributions of loamy sediments: a comparative study of ten instruments for wet analysis

Granja, H., De Groot, T. & Costa, A, Sedimentology **55** (2008), pp. 1203-1226:
Evidence for Pleistocene wet Aeolian dune and interdune accumulation, S. Pedro da Maceda, north-west Portugal

Sun, D., Bloemendal, J., Rea, D., Vandenberghe, J., Jiang, F., An, Z. & Su, R., Sedimentary Geology **152** (2002), pp. 263-277:
Grain-size distribution function of polymodal sediments in hydraulic and Aeolian environments, and numerical partitioning of the sedimentary components

Verlinden, V. & Hoogendoorn, R., *Sedimentary Dynamics and Coastal Development of the Eastern Section of the North Caspian Sea*, August 2009

Williamson, M., Practicing Oil Analysis (July 2002):
The Low-Down on Particle Counters

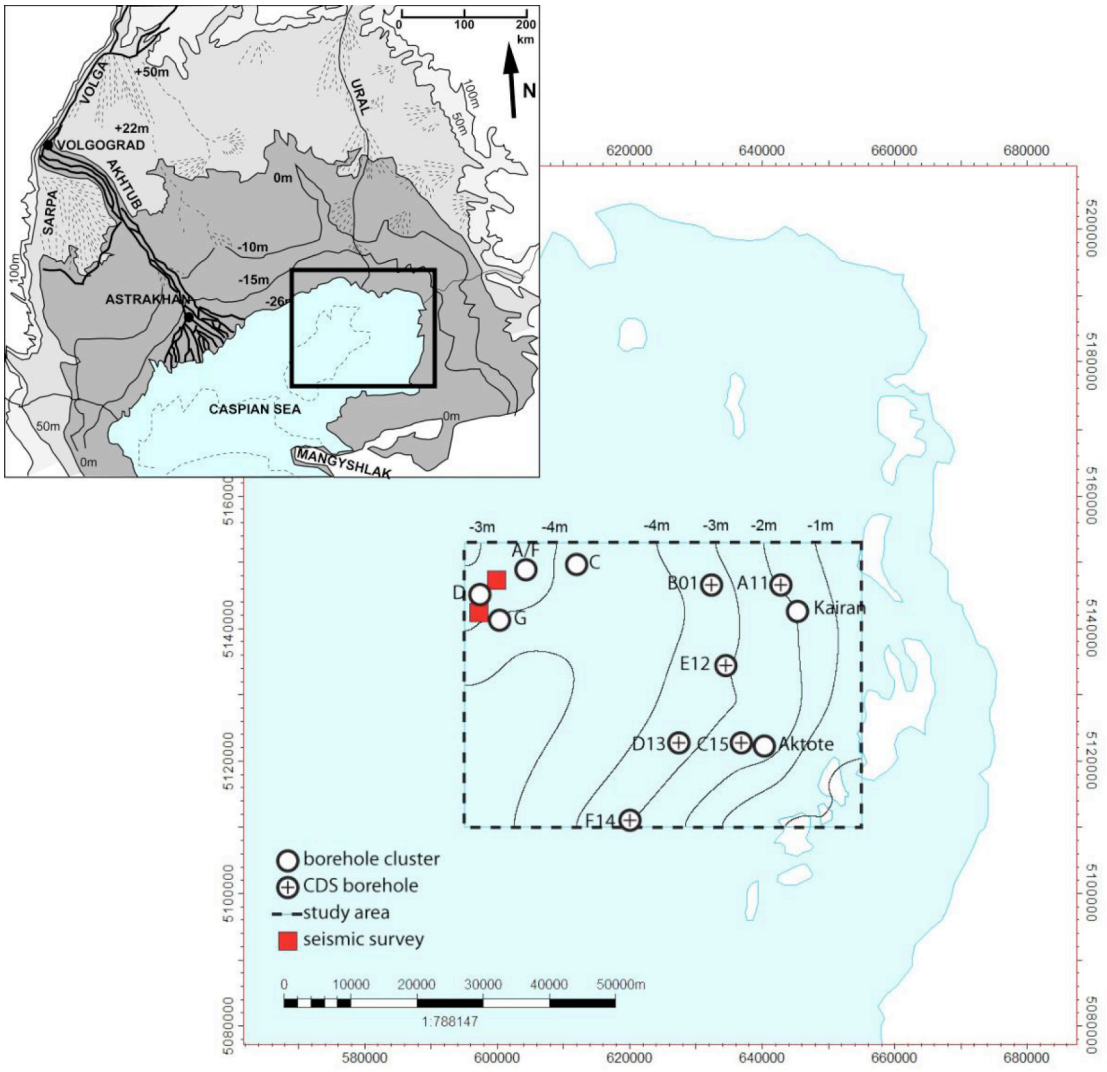

Figure 1
The central map shows the study area and the location of the 6 boreholes (CDSA – CDSF). The inset shows the general location of the study area in relation to the North Caspian Basin.
Source: Verlinden, V. & Hoogendoorn, R., *Sedimentary Dynamics and Coastal Development of the Eastern Section of the North Caspian Sea*, August 2009

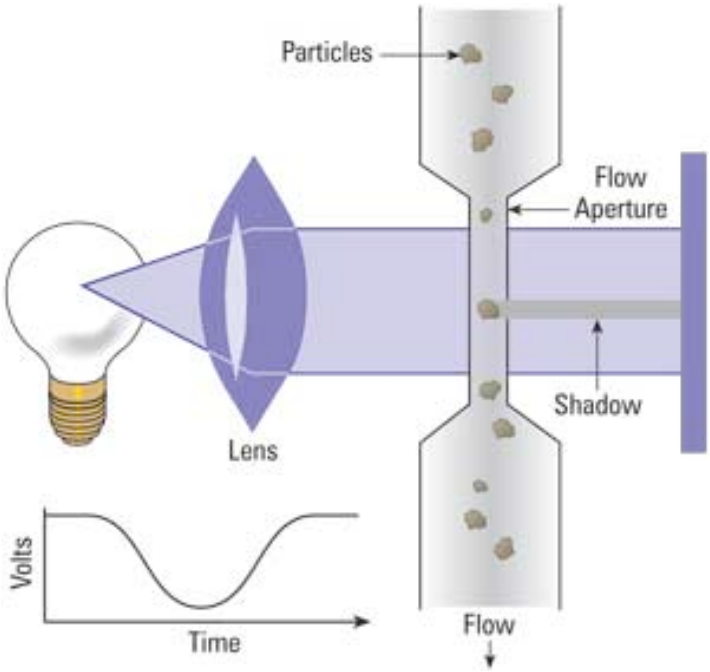

Figure 2
Schematic overview of a light blockage particle counter
Source: Williamson, M. (2002)

Udden–Wentworth	ϕ *values*	*German scale*† *(after Atterberg)*	*USDA and Soil Sci. Soc. Amer.*	*U.S. Corps Eng., Dept. Army and Bur. Reclamation*‡
		(Blockwerk)		
Cobbles		—200 mm—	Cobbles	Boulders
			—80 mm—	—10 in.—
—64 mm—	−6			Cobbles
Pebbles		Gravel (Kies)		—3 in.—
—4 mm—	−2		Gravel	Gravel
Granules				—4 mesh—
				Coarse sand
—2 mm—	−1	—2 mm—	—2 mm—	—10 mesh—
Very coarse sand			Very coarse sand	
—1 mm—	0		—1 mm—	
Coarse sand		Sand	Coarse sand	Medium sand
—0.5 mm—	1		—0.5 mm—	—40 mesh—
Medium sand			Medium sand	
—0.25 mm—	2		—0.25 mm—	
Fine sand			Fine sand	Fine sand
—0.125 mm—	3		—0.10 mm—	
Very fine sand			Very fine sand	—200 mesh—
—0.0625 mm—	4	—0.0625 mm—		
			—0.05 mm—	
Silt		Silt		
			Silt	Fines
—0.0039 mm—	8			
		—0.002 mm—	—0.002 mm—	
Clay		Clay (Ton)	Clay	

Table 1
Various size grade scales in common use
Source: Blatt, H., Middleton, G. & Murray, R., Origin of Sedimentary Rocks

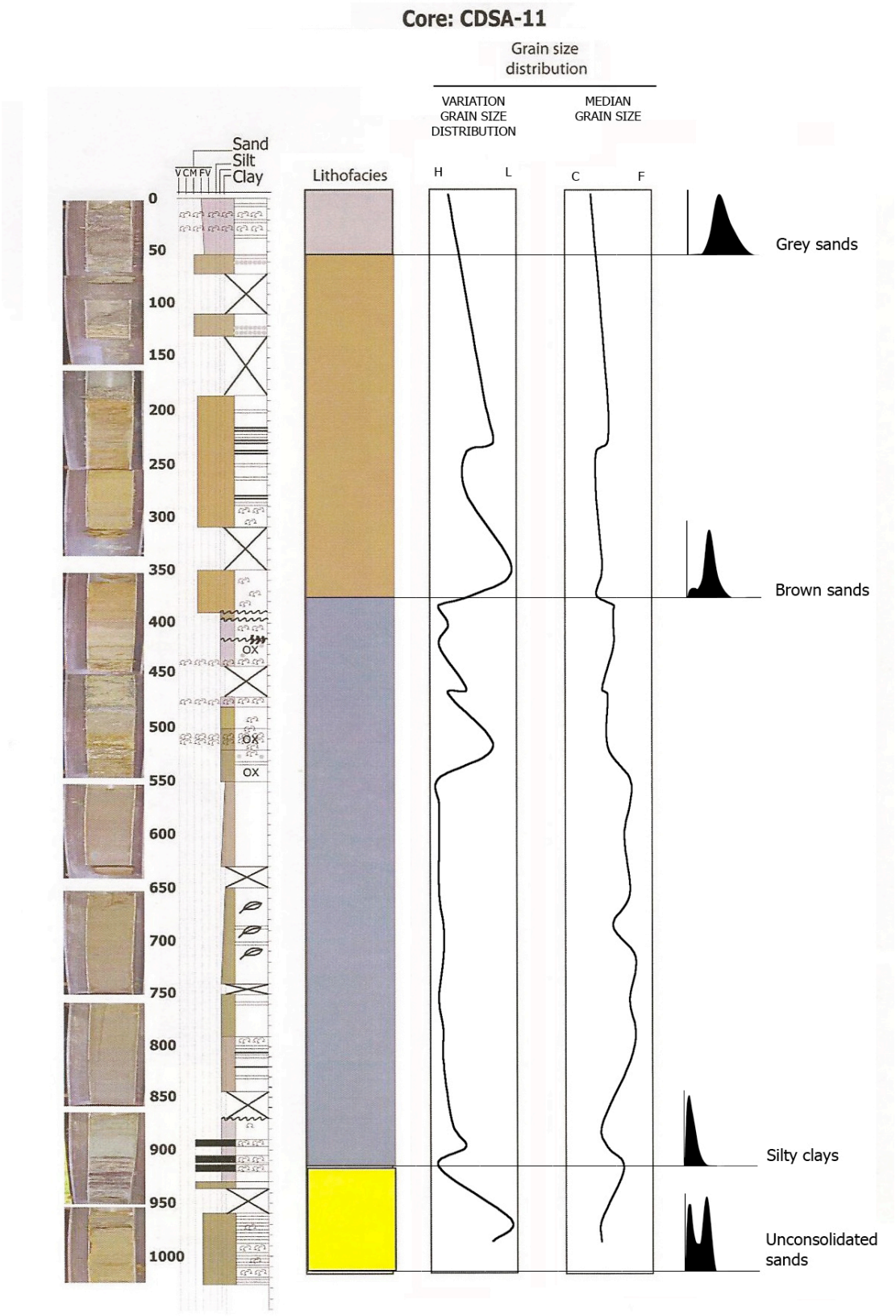
Core: CDSA-11
Grain size distribution
VARIATION GRAIN SIZE DISTRIBUTION
MEDIAN GRAIN SIZE
Sand
Silt
Clay
V C M F V
Lithofacies
H
L
C
F
0
50
100
150
200
250
300
350
400
450
500
550
600
650
700
750
800
850
900
950
1000
OX
OX
OX
Grey sands
Brown sands
Silty clays
Unconsolidated sands

Figure 3

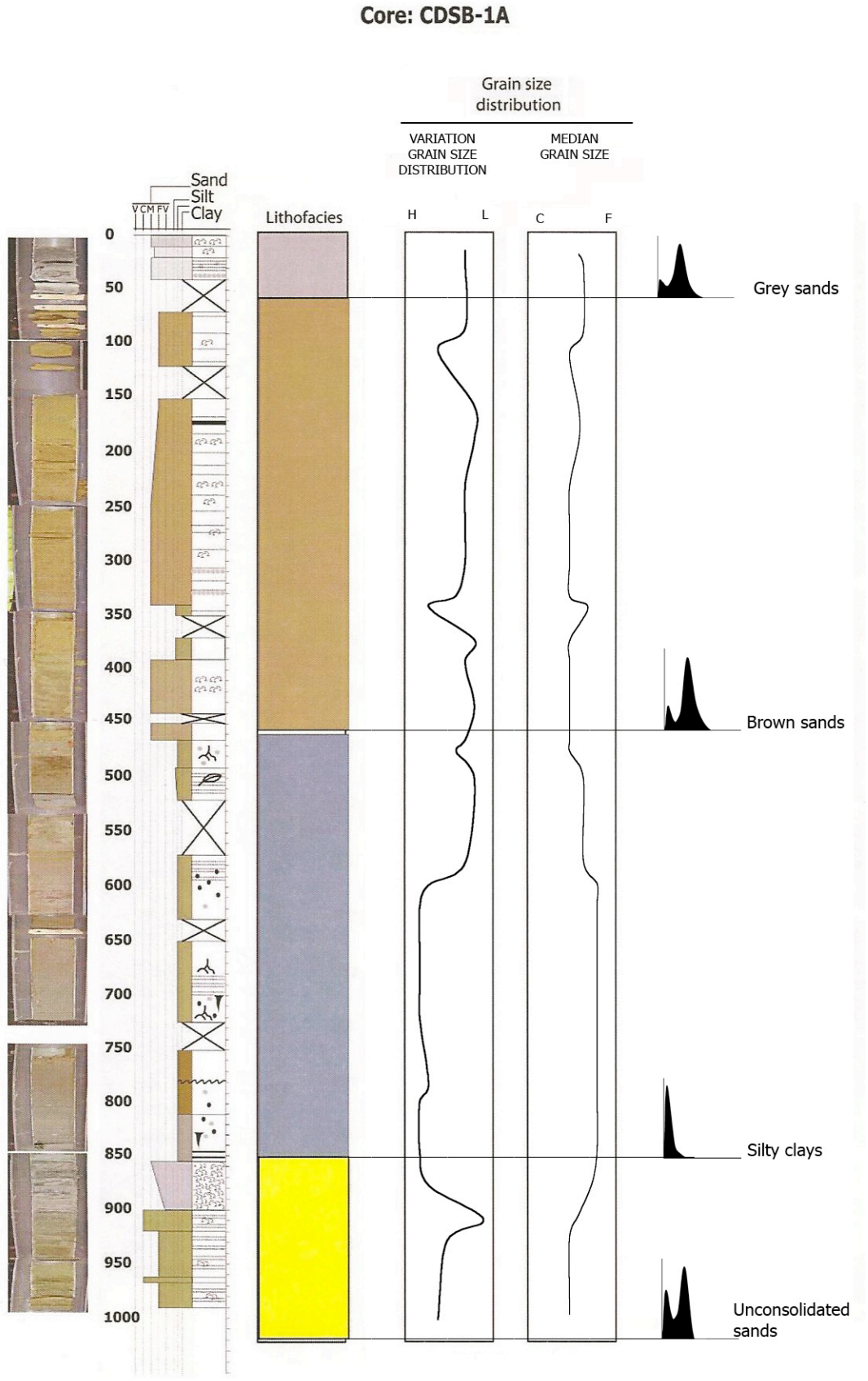
Core: CDSB-1A
Grain size distribution
VARIATION GRAIN SIZE DISTRIBUTION
MEDIAN GRAIN SIZE
Sand
Silt
Clay
V C M F V
Lithofacies
H
L
C
F
0
50
100
150
200
250
300
350
400
450
500
550
600
650
700
750
800
850
900
950
1000
Grey sands
Brown sands
Silty clays
Unconsolidated sands

Figure 4

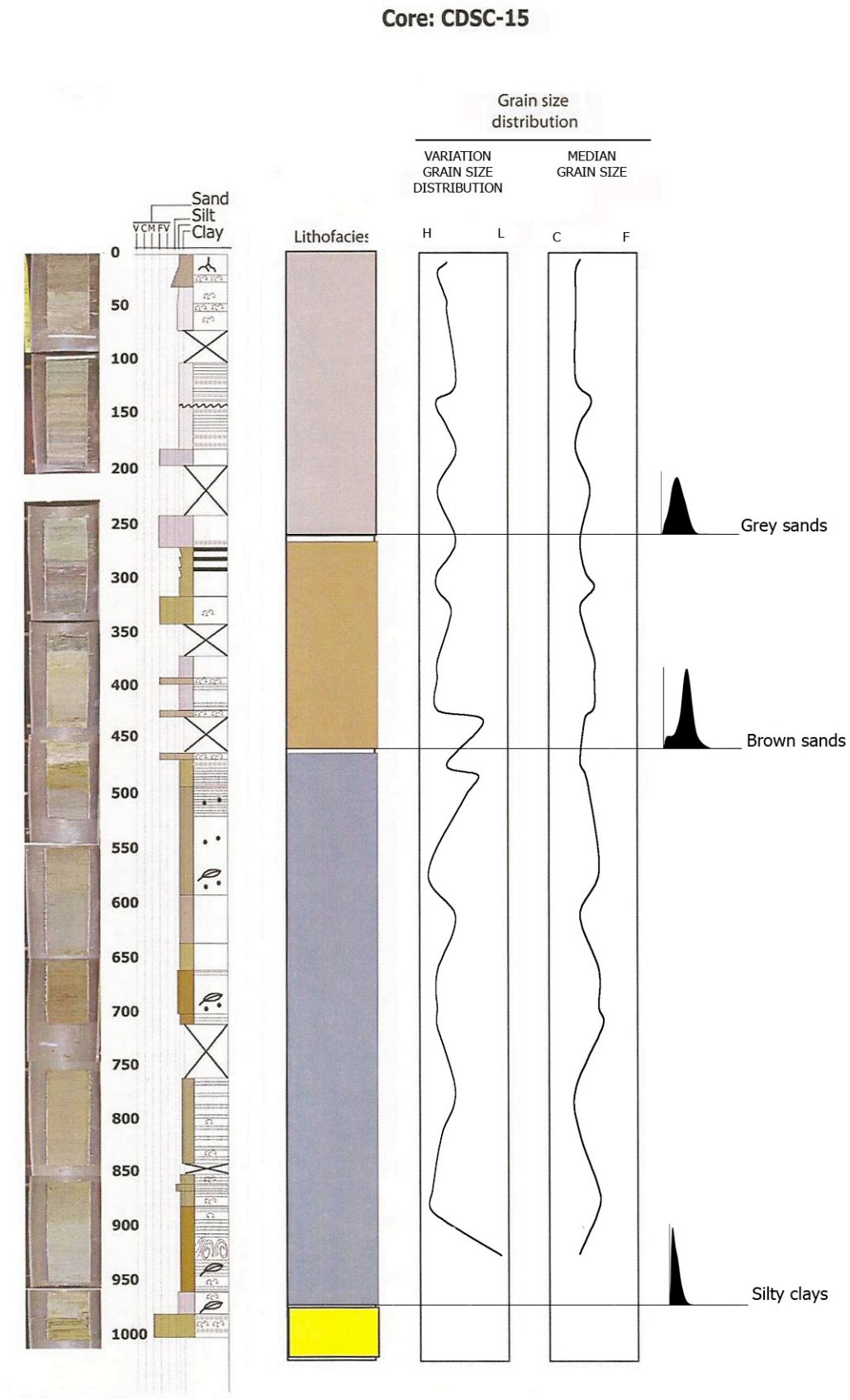
Core: CDSC-15
Grain size distribution
VARIATION GRAIN SIZE DISTRIBUTION
MEDIAN GRAIN SIZE
Sand
Silt
Clay
V C M F V
Lithofacies
H
L
C
F
0
50
100
150
200
250
300
350
400
450
500
550
600
650
700
750
800
850
900
950
1000
Grey sands
Brown sands
Silty clays

Figure 5

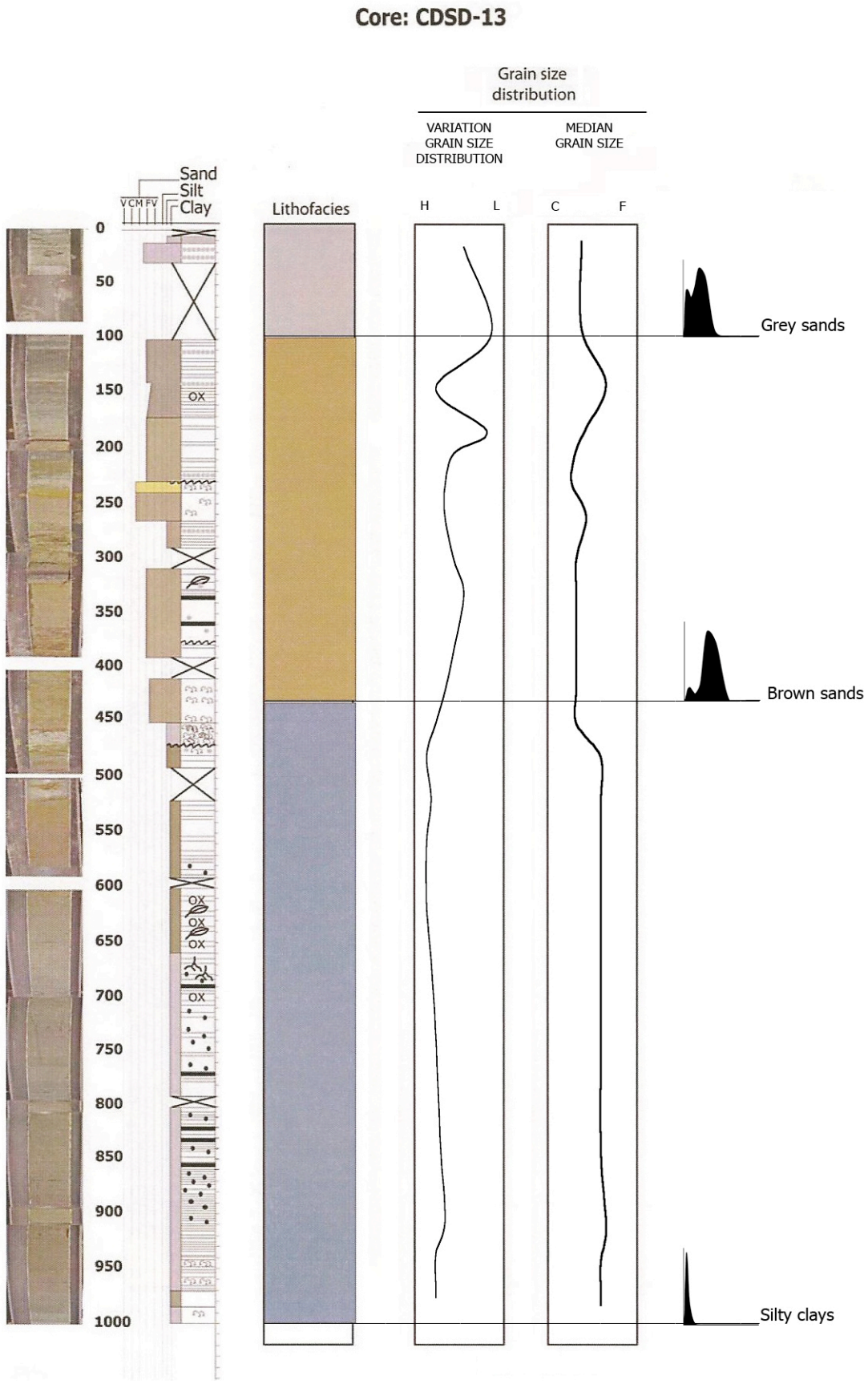
Core: CDSD-13
Grain size distribution
VARIATION GRAIN SIZE DISTRIBUTION
MEDIAN GRAIN SIZE
Sand
Silt
Clay
V C M F V
Lithofacies
H
L
C
F
0
50
100
150
200
250
300
350
400
450
500
550
600
650
700
750
800
850
900
950
1000
ox
Grey sands
Brown sands
Silty clays

Figure 6

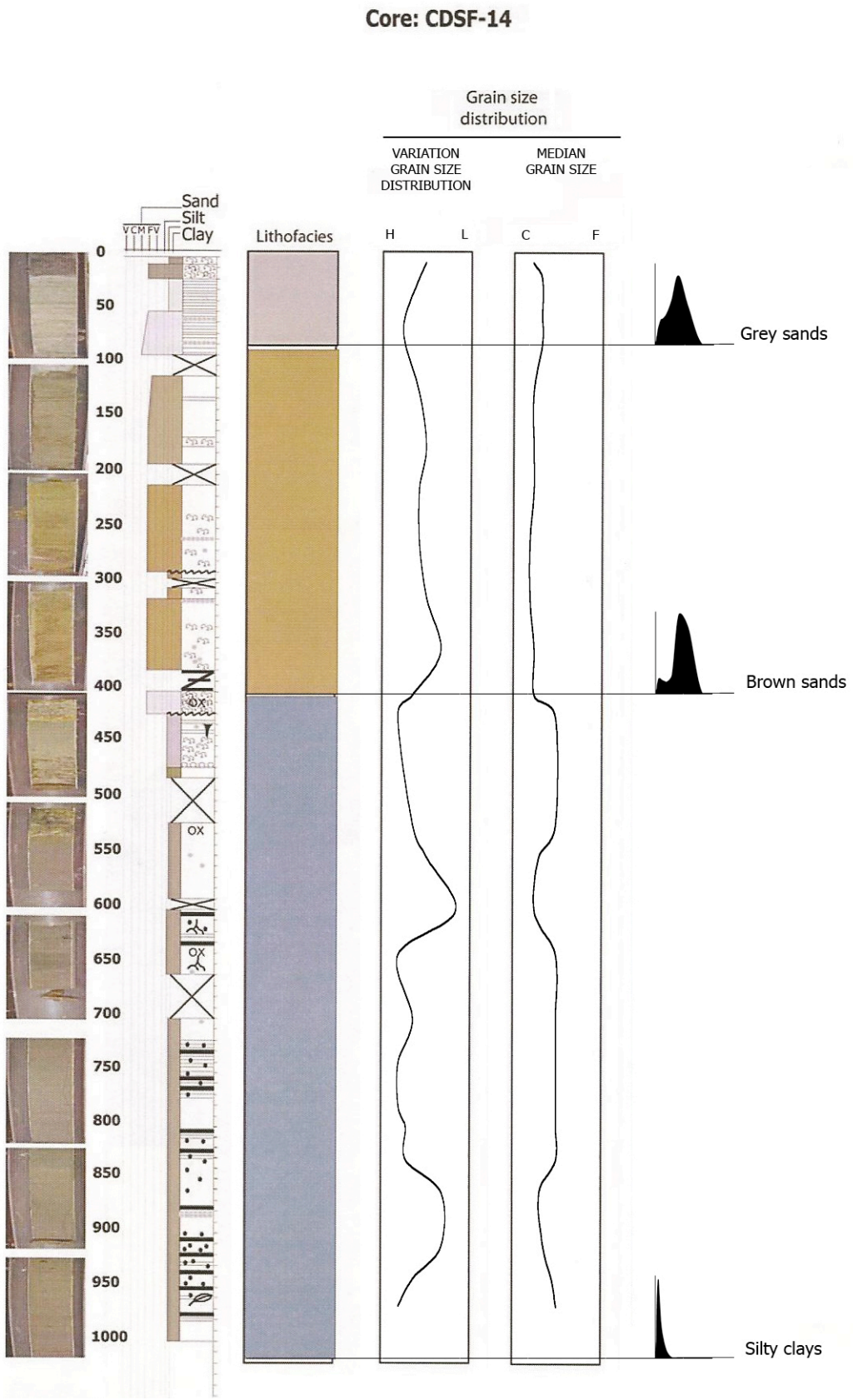
Core: CDSF-14
Grain size distribution
VARIATION GRAIN SIZE DISTRIBUTION
MEDIAN GRAIN SIZE
Sand
Silt
Clay
V C M F V
Lithofacies
H
L
C
F
0
50
100
150
200
250
300
350
400
450
500
550
600
650
700
750
800
850
900
950
1000
OX
Grey sands
Brown sands
Silty clays

Figure 7